

# Insulation Characteristics of Gas Mixtures including Perfluorocarbon Gas

Masayuki Hikita, Shinya Ohtsuka

Kyushu Institute of Technology  
Department of Electrical Engineering  
1-1 Sensui-cho, Tobata-ku, Kitakyushu, Fukuoka, 804-8550, Japan

Shigemitsu Okabe and Shuhei Kaneko

Tokyo Electric Power Company  
R & D Center, High Voltage & Insulation Group  
4-1, Egasaki-cho, Tsurumi-ku, Yokohama, Kanagawa, 230-8510, Japan

## ABSTRACT

This paper describes discharge properties of  $N_2$  and  $CO_2$ -based gas mixtures including a perfluorocarbon (PFC) gas such as  $CF_4$ ,  $C_3F_8$  and  $c-C_4F_8$  under non-uniform field. The mixture ratio between a base gas of  $N_2$  or  $CO_2$  and the additive PFC gas was fixed as 9:1; namely, 90% $N_2$ /10%PFC or 90% $CO_2$ /10%PFC gas mixture. The PFC gases have even smaller global warming potential (GWP) than  $SF_6$  gas and have good insulation properties as  $SF_6$  gas. Thus, PFC gas mixture is expected to be a  $SF_6$  substitute without highly pressurizing the gas over the conventional pressure of 0.5 to 0.6 MPa. In this study, in order to compare the partial discharge (PD) inception voltage  $V_{PD}$  and breakdown voltage  $V_B$  properties between  $N_2$  and  $CO_2$ -based gas mixtures, as well as between the additive gas of PFC and  $SF_6$  gas, we investigated these properties of the gas mixtures with a needle to plane electrode under ac high voltage application. The gas pressure was changed from 0.1 to 0.6 MPa. As a result, it was found that  $V_{PD}$  and  $V_B$  characteristics of  $N_2$  and  $CO_2$ -based gas mixtures differed considerably, especially the gas pressure dependence of  $V_B$  (so-called the  $N$  shape characteristics).  $V_B$  characteristics of  $N_2$ -based gas mixture including  $c-C_4F_8$  proved to be excellent within the test conditions over the wide gas pressure region, showing the maximum breakdown voltage. In terms of  $V_{PD}$  properties,  $CO_2$ -based gas mixture had an advantage over  $N_2$ -based gas mixture due to higher  $V_{PD}$ . Furthermore, we discussed the synergy effects of  $V_{PD}$  and  $V_B$  for  $N_2$  and  $CO_2$ -based gas mixtures using the index  $R_n$  which was defined to quantify the degree of the effect.  $R_n$  for  $CO_2$ -based gas mixture was higher than that of  $N_2$ -based gas mixture.

Index Terms —  $SF_6$  gas, perfluorocarbon (PFC) gas, partial discharge, breakdown voltage, non-uniform field.

## 1 INTRODUCTION

SINCE  $SF_6$  gas has excellent insulation and arc-quenching properties, it has been widely used as insulation media for gas insulated switchgear (GIS) and gas insulated transmission line (GIL). However,  $SF_6$  gas is a potent green house gas with global warming potential (GWP) as large as 23,900. Thus, the decrease in the use of  $SF_6$  gas and the development of the alternative gas having much lower GWP are required [1-3]. From this point of view, a lot of experimental and numerical studies have been made on gas mixtures which are composed of a small amount of an electronegative gas such as  $SF_6$  and a perfluorocarbon

(PFC) gas, mixed with a buffer gas like  $N_2$ ,  $CO_2$  and air as a base gas to avoid the gas pressure to be extremely high over 1.0 MPa [1-9]. High pressure gas requires quite a thick tank wall and it could compel GIS to need highly cost and weight, in addition, the equipments with over 1.0 MPa pressured gas are severely regulated in Japan. PFC gas has the advantage of GWP, which is one order of magnitude smaller than that of  $SF_6$ , and the dielectric strength is almost same as that of  $SF_6$  [3, 4, 6-8]. So far, the authors have investigated insulation properties of  $CO_2/N_2/SF_6$  ternary gas mixtures under non-uniform as well as uniform field by applying ac and standard lightning impulse voltages [9]. Using the same experimental setup and techniques, discharge properties of  $N_2$  and  $CO_2$ -based gas mixtures including PFC gas can be investigated.

Manuscript received on 20 September 2007, in final form 24 January 2008.

In this study, in order to discuss the difference in PD inception voltage  $V_{PD}$  and breakdown voltage  $V_B$  characteristics not only between  $N_2$  and  $CO_2$ -based gas mixtures, but also between the additive gas of PFC and  $SF_6$  gas, we experimentally investigated  $V_{PD}$  and  $V_B$  characteristics of these gas mixtures under non-uniform field by ac high voltage application. Synergism effect of  $SF_6$  gas mixture could be observed remarkably with only 2% to 10% proportion of  $SF_6$  [10]. In the experiment of this study, from this reason, the mixture ratio of a base  $N_2$  or  $CO_2$  gas to the additive PFC or  $SF_6$  gas was fixed as 9:1, i.e., 90% $N_2$ /10%PFC or 90% $CO_2$ /10%PFC gas mixture. We used  $CF_4$ ,  $C_3F_8$  and  $c-C_4F_8$  gases as an additive PFC gas. Additionally, the synergy effects on  $V_{PD}$  and  $V_B$  for these gas mixtures were discussed by introducing the index  $R_n$ , that is defined to quantify the degree of the effect.

## 2 EXPERIMENTAL SETUP AND PROCEDURE

Figure 1 shows schematic diagram of experimental setup to investigate discharge properties of the gas mixtures including a PFC gas under non-uniform field. Tested gas mixtures consist of a PFC gas such as  $CF_4$ ,  $C_3F_8$  and  $c-C_4F_8$  and a base gas of  $N_2$  or  $CO_2$ . Specifications of each component gas are listed in Table 1. The mixture ratio of each component gas was decided by the pressure ratio of each gas at room temperature. The mixture ratio of a base gas to a PFC gas was fixed as 9:1; i.e. the mixture rate of a PFC gas was 10%. Prior to use for experiment, the gas mixtures were left for 24 h after mixing. A needle to plane electrode system made of stainless steel was mounted in a pressure chamber. The tip radius of the needle electrode was 500  $\mu m$  and the gap length between electrodes was

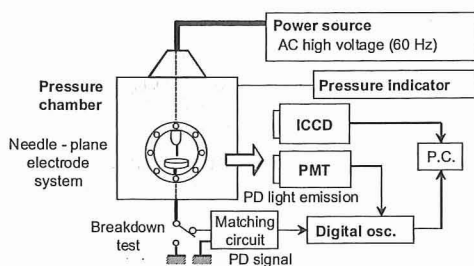


Figure 1. Experimental setup.

Table 1. Specifications of component gases used experiments [4,5].

| Gas        | GWP (100 years) | Vapor pressure (MPa)     | Boiling temperature ( $^{\circ}C$ ) | Relative strength <sup>*1</sup> |
|------------|-----------------|--------------------------|-------------------------------------|---------------------------------|
| $CF_4$     | 6,500           | *2                       | -128                                | 0.43                            |
| $C_3F_8$   | 7,000           | 0.78 (21.1 $^{\circ}C$ ) | -38                                 | 0.93                            |
| $c-C_4F_8$ | 8,700           | 0.29 (24.3 $^{\circ}C$ ) | -8                                  | 1.3 - 1.4                       |
| $SF_6$     | 23,900          | 2.28 (21.1 $^{\circ}C$ ) | -64                                 | 1.0                             |
| $N_2$      | -               | *3                       | -196                                | 0.40                            |
| $CO_2$     | 1               | 5.75 (21.1 $^{\circ}C$ ) | -79                                 | 0.37                            |

\*1)Uniform field, \*2)Compressed gas at room temperature, \*3)Critical temperature -147.1 $^{\circ}C$ .  $N_2$  can not be liquefied at temperatures higher than this.

maintained as 10 mm in all experiments. Note that the electric non-uniform coefficient of this system is 14.5.

$V_{PD}$  and  $V_B$  characteristics of the gas mixtures were investigated by applying ac high voltage (60 Hz) to the needle electrode in the gas pressure range from 0.1 to 0.6 MPa. PD signal was detected with a digital oscilloscope (1GHz, 4Gs/s) through an impedance matching circuit connected between the plane electrode and earth ground [9]. When  $V_B$  was measured, the matching circuit was removed and the plane electrode was directly grounded for protecting the electronic devices. PD light emission intensity and image were measured by PMT (Photomultiplier Tube) and ICCD (Intensified Charge-coupled Devices) camera, respectively.

## 3 EXPERIMENTAL RESULTS

### 3.1 DISCHARGE PROPERTIES OF UNITARY PFC AND BUFFER GAS

Figure 2 shows positive  $V_{PD}$  ( $V_{PD}^+$ ) and  $V_B$  characteristics of  $SF_6$ ,  $N_2$  and  $CO_2$  as a function of gas pressure [9]. Although not showing in Figure 2, experimental results revealed that negative  $V_{PD}$  ( $V_{PD}^-$ ) for these gases were lower than  $V_{PD}^+$ . It is obvious from Figure 2 that  $V_B$  of  $N_2$  linearly increases with gas pressure due to inherent nature of the non-electronegative gas. On the other hand,  $V_{BS}$  of  $SF_6$  and  $CO_2$  do not show the linearity to the gas pressure but the well-known  $N$  shape characteristics, which are caused by the corona stabilization effect. The electronegative gases, i.e.,  $SF_6$  and  $CO_2$ , are easy to ionize negatively. Since the electrons are known to attach to molecules in electronically excited states with higher probability than to molecules in the ground electronic states, the ionized molecules would contribute to an enhancement in the breakdown voltage [1, 2]. Both  $V_{PD}^+$  and  $V_B$  increase in order of  $N_2$ ,  $CO_2$  and  $SF_6$ . The results for  $N_2$  and  $CO_2$  differ from those obtained under the uniform field as listed in Table 1 [4, 5]. Namely, dielectric strength of  $N_2$  is larger than that of  $CO_2$  under uniform field. One reason for this difference in  $V_{PD}^+$  seems to come from the detection sensitivity of PD current signal through the impedance matching circuit shown in Figure 1.

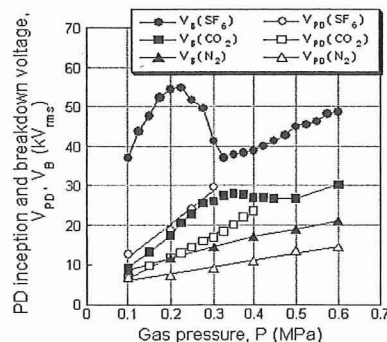


Figure 2. Positive  $V_{PD}$  and  $V_B$  characteristics of unitary gases of  $N_2$ ,  $CO_2$  and  $SF_6$  gas [9].

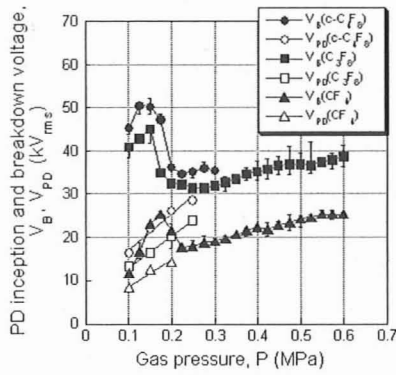


Figure 3. Positive  $V_{PD}$  and  $V_B$  characteristics of unitary PFC gases of  $CF_4$ ,  $C_3F_8$  and  $c-C_4F_8$ .

Figure 3 depicts schematic gas pressure dependence of  $V_{PD+}$  and  $V_B$  for unitary PFC gases of  $CF_4$ ,  $C_3F_8$  and  $c-C_4F_8$ . These voltage characteristics for  $c-C_4F_8$  were measured below 0.3MPa to avoid liquefying the gas. The  $N$  shape characteristics of  $V_B$  are confirmed in all PFC gases like  $SF_6$  and  $CO_2$  gas shown in Figure 2.  $V_{PD}$ -s for PFC gases were also found to be lower than  $V_{PD+}$ . Here, let us define the maxima and minima in a  $V_B$  vs  $P$  curve as  $V_{Bm}$  and  $V_{C'}$ , and also define the corresponding gas pressures as  $P_m$  and  $P_{C'}$ , as shown in Figure 4, respectively [9]. These parameters as well as  $V_{PD+}$  and  $V_{PD-}$  at 0.2 MPa of the tested unitary gases shown in Figures 2 and 3 are listed in Table 2.  $V_{PD+}$  as well as  $V_B$  rise in order of  $CF_4$ ,  $C_3F_8$  and  $c-C_4F_8$ , which is the same order as for the case under the uniform field listed in Table 1. Particularly, it should be noticed that the normalized  $V_{PD+}$  and  $V_{PD-}$  for  $C_3F_8$ ,  $c-C_4F_8$  and  $N_2$  against  $SF_6$  listed in Table 2 are nearly equal to the normalized strength under the uniform field (Table 1). On the other hand, the normalized  $V_{Bs}$  for these gases listed in Table 2 do not agree with the relative strength under the uniform field because of the influence of the space charge by PD. This result shows that  $V_{PD}$  is closely related to the dielectric strength under the uniform field. It is also found from Table 2 that  $P_m$  for PFC gas appears at lower gas pressure than that for  $SF_6$ . Figure 5 shows molecular weight dependences of  $V_{PD+}$ ,  $V_{PD-}$  and  $V_B$  at 0.1 MPa for all tested gases. This result indicates that  $V_{PD}$  and  $V_B$  increase with the molecular

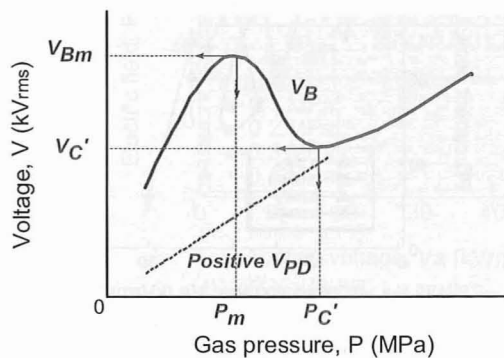


Figure 4. Definition of  $V_{Bm}$ ,  $V_{C'}$ ,  $P_m$  and  $P_{C'}$  in the  $N$  shape characteristics of  $V_B$  vs  $P$  curve.

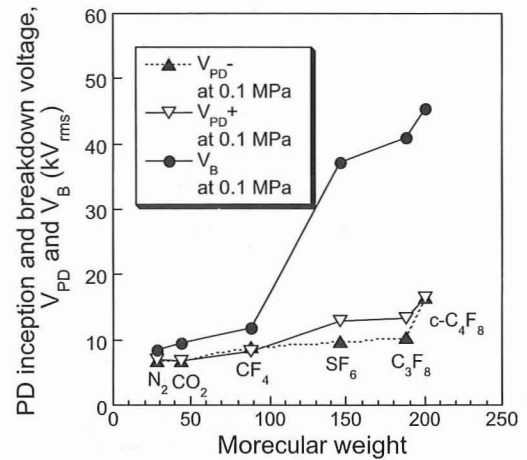


Figure 5. Molecular weight dependence of insulation properties of each unitary gas shown in Figures 2 and 3.

Table 2. Specifications of PFC gases shown in Figures 2 and 3.  $V_{PD}$ ,  $V_{Bm}$  and  $V_{C'}$  are relative values to that of  $SF_6$ .

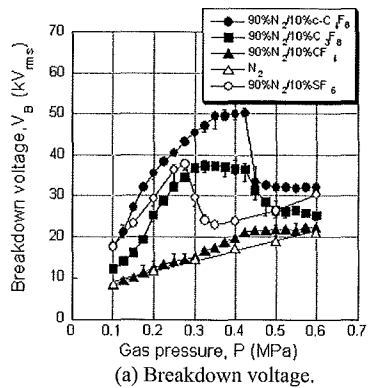
| Mixed gas  | $V_{PD+}$ at 0.2 MPa | $V_{PD-}$ at 0.2 MPa | $V_{Bm}$ | $P_m$ (MPa) | $V_{C'}$ | $P_{C'}$ (MPa) |
|------------|----------------------|----------------------|----------|-------------|----------|----------------|
| $CF_4$     | 0.76                 | 0.84                 | 0.46     | 0.175       | 0.47     | 0.225          |
| $C_3F_8$   | 1.08                 | 1.02                 | 0.82     | 0.15        | 0.85     | 0.25           |
| $c-C_4F_8$ | 1.40                 | 1.24                 | 0.92     | 0.125       | 0.93     | 0.225          |
| $SF_6$     | 1.0                  | 1.0                  | 1.0      | 0.225       | 1.0      | 0.325          |
| $N_2$      | 0.40                 | 0.42                 | -        | -           | -        | -              |
| $CO_2$     | 0.63                 | 0.65                 | 0.51     | 0.35        | 0.72     | 0.5            |

weight, and the difference between  $V_B$  and  $V_{PD}$ ; i.e. corona stabilization effect, also increases with the molecular weight.

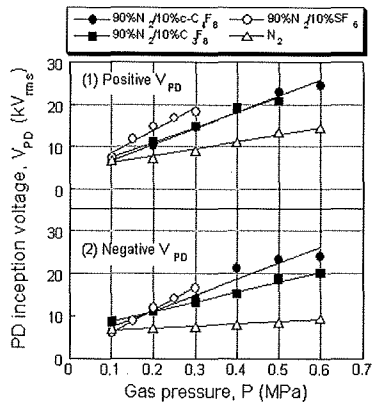
### 3.2 DISCHARGE PROPERTIES OF $N_2$ /PFC AND $CO_2$ /PFC GAS MIXTURES

$V_{PD}$  and  $V_B$  of 90% $N_2$ /10%PFC and 90% $CO_2$ /10%PFC gas mixtures as a function of the gas pressure are shown in Figures 6 and 7, respectively.  $V_{PD}$  for  $N_2/CF_4$  gas mixture could not be measured because  $V_{PD}$  was close to  $V_B$ . Although  $V_B$  vs  $P$  curves of both  $N_2$ /PFC and  $CO_2$ /PFC gas mixtures indicate the  $N$  shape characteristics,  $V_B$  vs  $P$  curves for  $N_2$ /PFC gas mixtures quite differ from those for  $CO_2$ /PFC ones; that is,  $V_{Bm}$  for  $N_2$ /PFC gas mixtures, particularly including  $C_3F_8$  and  $c-C_4F_8$ , appears at higher gas pressures than that for  $CO_2$ /PFC ones. Also, we can say that the  $N$  shape curves of  $V_B$  for  $CO_2$ /PFC gas mixture seem to be similar with that for  $CO_2/SF_6$  one, while those for  $N_2$ /PFC gas mixture differs from that for  $N_2/SF_6$  one as mentioned above. This relation is also confirmed quantitatively in Tables 3 and 4, which list the parameters of the gas mixtures shown in Figures 6 and 7. It should be noted that  $P_m$  for the PFC gas mixtures shifts to higher gas pressure compared with pure PFC gas.

Some differences in  $V_{PD}$  properties between  $N_2$ /PFC and  $CO_2$ /PFC gas mixtures were also confirmed in Figures 6 and 7. Namely,  $V_{PD}$  for  $CO_2$ /PFC gas mixtures are generally higher than that for  $N_2$ /PFC ones, and difference between

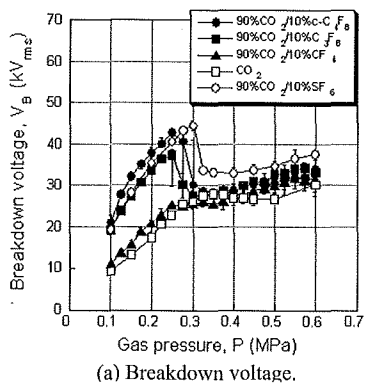


(a) Breakdown voltage.

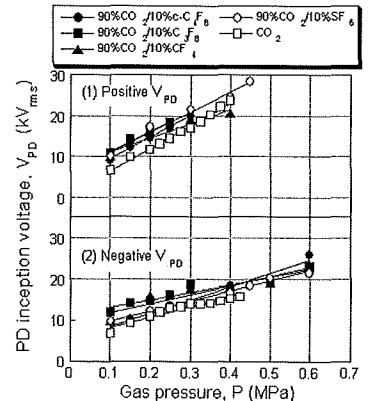


(b) Positive and negative PD inception voltage.

Figure 6. Discharge properties of 90%N<sub>2</sub>/10%PFC gas mixtures.



(a) Breakdown voltage.



(b) Positive and negative PD inception voltage.

Figure 7. Discharge properties of 90%CO<sub>2</sub>/10%PFC gas mixtures.

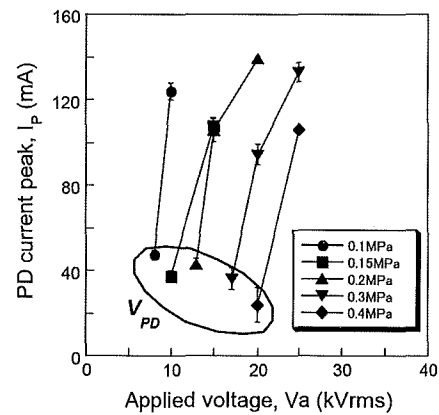
$V_{PD+}$  and  $V_{PD-}$  for CO<sub>2</sub>/PFC gas mixtures seems to be slightly larger than that for N<sub>2</sub>/PFC ones; e.g.  $V_{PD+}$  of N<sub>2</sub>/c-C<sub>4</sub>F<sub>8</sub> gas mixture is identical to the  $V_{PD-}$ . Thus, from the viewpoint of  $V_{PD}$ , CO<sub>2</sub>/PFC gas mixtures have an advantage over N<sub>2</sub>/PFC ones due to higher  $V_{PD}$  although the peak value of the PD current pulses of CO<sub>2</sub>/PFC gas mixtures generated during the positive half cycle indicates higher value than that of N<sub>2</sub>/PFC ones as shown in Figure 8. Corona stabilization effect gives larger PD current with  $V_a$

Table 3. Parameters of 90%N<sub>2</sub> gas mixtures shown in Figure 6.

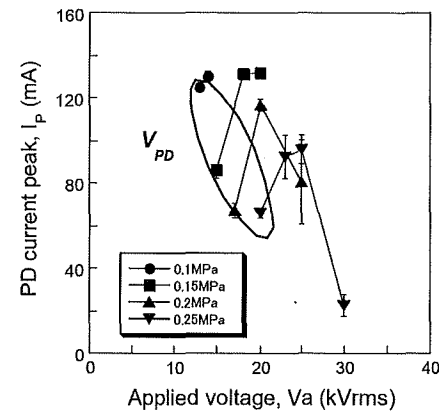
| Mixed gas                       | $V_{PD+}$ at 0.2 MPa | $V_{PD-}$ at 0.2 MPa | $V_{Bm}$ | $P_m$ (MPa) | $V_c'$ | $P_c'$ (MPa) |
|---------------------------------|----------------------|----------------------|----------|-------------|--------|--------------|
| CF <sub>4</sub>                 | -                    | -                    | 0.57     | 0.45        | 0.94   | 0.55         |
| C <sub>3</sub> F <sub>8</sub>   | 0.76                 | 0.94                 | 0.99     | 0.35        | 1.14   | 0.525        |
| c-C <sub>4</sub> F <sub>8</sub> | 0.69                 | 0.95                 | 1.33     | 0.425       | 1.40   | 0.5          |
| SF <sub>6</sub>                 | 1.0                  | 1.0                  | 1.0      | 0.275       | 1.0    | 0.35         |

Table 4. Parameters of 90%CO<sub>2</sub> gas mixtures shown in Figure 7.

| Mixed gas                       | $V_{PD+}$ at 0.2 MPa | $V_{PD-}$ at 0.2 MPa | $V_{Bm}$ | $P_m$ (MPa) | $V_c'$ | $P_c'$ (MPa) |
|---------------------------------|----------------------|----------------------|----------|-------------|--------|--------------|
| CF <sub>4</sub>                 | 0.92                 | 1.31                 | 0.57     | 0.25        | 0.78   | 0.35         |
| C <sub>3</sub> F <sub>8</sub>   | 0.95                 | 1.20                 | 0.84     | 0.25        | 0.83   | 0.3          |
| c-C <sub>4</sub> F <sub>8</sub> | 0.84                 | 0.87                 | 0.96     | 0.25        | 0.86   | 0.35         |
| SF <sub>6</sub>                 | 1.0                  | 1.0                  | 1.0      | 0.30        | 1.0    | 0.40         |



(a) 90%N<sub>2</sub>/10%PFC gas mixtures.



(b) 90%CO<sub>2</sub>/10%PFC gas mixtures.

Figure 8. Applied voltage dependence of the peak value of PD current pulses during the positive half cycle for different gas pressures.

in Figure 8 but for CO<sub>2</sub>/PFC gas mixture, some data points with higher gas pressure show decline trend with V<sub>a</sub> where the gas pressure correspond to the range of being shift to the no corona stabilization region.

### 3.3 PARTIAL DISCHARGE LIGHT EMISSION PROPERTIES OF N<sub>2</sub>/PFC AND CO<sub>2</sub>/PFC GAS MIXTURES

As an example of difference in PD properties between N<sub>2</sub>/PFC and CO<sub>2</sub>/PFC based gas mixture, we observed PD light emission images of the 90%N<sub>2</sub>/10%C<sub>3</sub>F<sub>8</sub> and 90%CO<sub>2</sub>/10%C<sub>3</sub>F<sub>8</sub> gas mixtures.

Figures 9a to 9d display photos of PD light emission images of 90%N<sub>2</sub>/10%C<sub>3</sub>F<sub>8</sub> and 90%CO<sub>2</sub>/10%C<sub>3</sub>F<sub>8</sub> gas mixtures together with N<sub>2</sub> and CO<sub>2</sub> unitary gas at (1) 0.15 MPa and around (2) P<sub>m</sub>. All of the photos were taken by an accumulated exposure time of 20 μs near the phase angle of 90deg. of the alternating voltage, i.e. positive peak. As shown in these photos, PD light emission images reflect that of the base gas. Namely, PDs of CO<sub>2</sub>/C<sub>3</sub>F<sub>8</sub> gas mixture emit light in such a way that the light wraps the tip of the needle electrode irrespective of the gas pressure as in Figure 9b. On the other hand, in the low pressure range below P<sub>m</sub> of

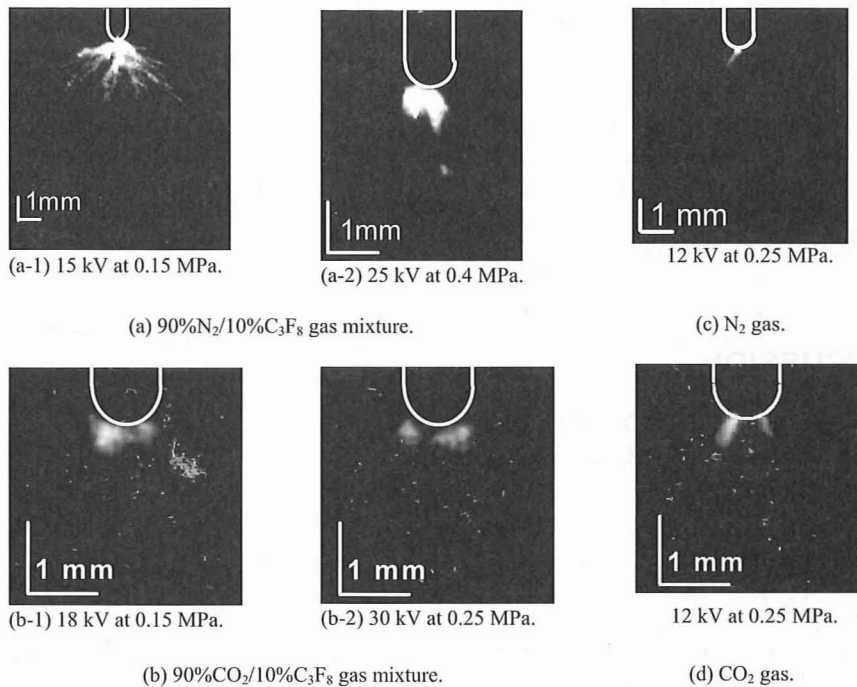


Figure 9. PD light images for tested gas mixtures.

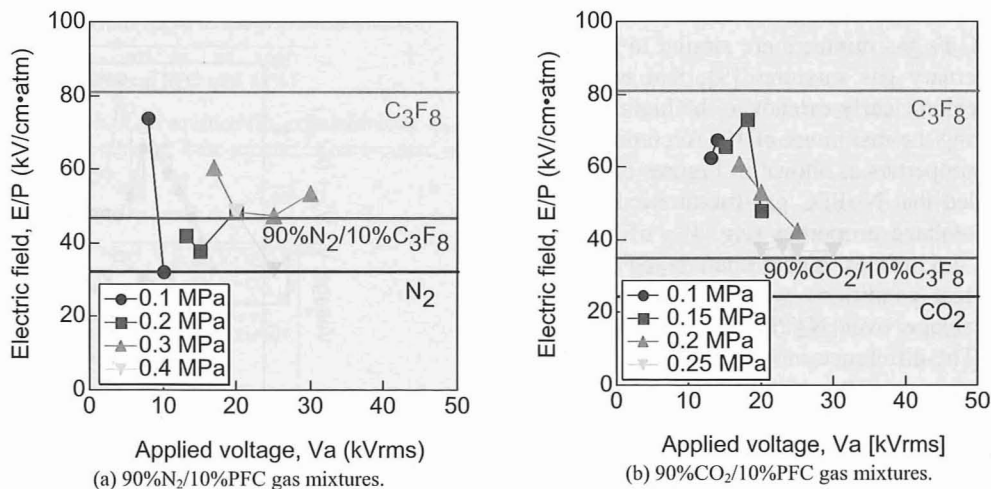


Figure 10. Applied voltage dependence of the reduced electric field strength calculated at the tip of the PD light emission images for different gas pressures. The three lines in each figure represent the reduced critical field of each gas.

the  $N_2/C_3F_8$  gas mixture, tree-like PD light emission pattern is observed as in Figure 9a-1 which is characterized by the  $N_2$  unitary gas as in Figure 9c. In the high pressure region above  $P_m$ , filamentary light characterized by leader discharges appears out of the light surrounding the needle tip as in Figure 9a-2.

Here, we indicated the applied voltage dependence of the reduced electric field strength calculated at a position where the PD stops. The space charge effect was not considered throughout the calculation. The term "critical field" in Figure 10 is defined as that the effective ionization coefficient is absolutely zero. The horizontal line in Figure 10a and 10b represents the reduced critical field strength for each gas. Note that PD in  $90\%CO_2/10\%C_3F_8$  gas mixture develops up to the critical field of the mixture gas while PD in  $90\%N_2/10\%C_3F_8$  gas mixture further develops to the critical field of the base gas ( $N_2$ ). As the reduced critical field of  $N_2$  is lower than that of  $90\%CO_2/10\%C_3F_8$  gas mixture, these PD light emission development properties seem to result in lower  $V_{PD}$  of  $N_2/PFC$  gas mixtures compared with that of  $CO_2/PFC$  ones shown in Figures 6 and 7.

## 4 DISCUSSION

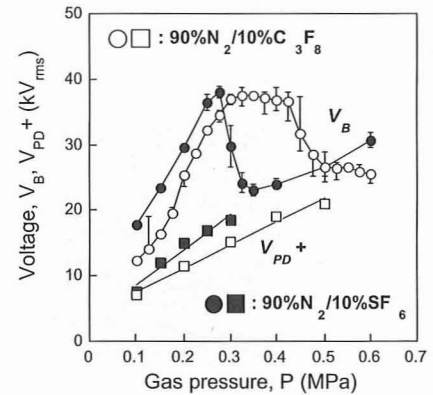
### 4.1 COMPARISON OF DISCHARGE PROPERTIES BETWEEN THE GAS MIXTURES INCLUDING PFC AND $SF_6$ GAS

Based on the results in Figures 6 and 7, we compared  $V_B$  and  $V_{PD}$  characteristics of the gas mixtures including PFC gas with those including  $SF_6$  gas. In  $CO_2$ -based gas mixtures,  $V_B$  of  $CO_2/c-C_4F_8$  gas mixture only exceeds that of  $CO_2/SF_6$  gas mixture below 0.25 MPa, which corresponds to  $P_m$  of  $CO_2/c-C_4F_8$  gas mixture. On the other hand,  $V_B$  of  $N_2/c-C_4F_8$  and  $N_2/C_3F_8$  gas mixtures exceeds that of  $N_2/SF_6$  gas mixture in the whole gas pressure region tested and above 0.275 MPa corresponding to  $P_m$  of  $N_2/SF_6$  gas mixture. As compared with Figures 11a to 11c,  $V_B$  characteristics of  $N_2/C_3F_8$  gas mixtures are similar to those of the  $CO_2/N_2/SF_6$  ternary gas mixtures [9]; that is, the corona stabilization region clearly extends to the higher gas pressures over  $P_m$  giving the maximum of  $V_B$ . According to these results and  $V_C'$  properties as shown in Figures 6a and 7a, it can be concluded that  $N_2/PFC$  gas mixture exhibits excellent breakdown voltage properties (e.g.  $V_{Bm}$  of  $N_2/c-C_4F_8$  gas mixture is 1.33 times higher than  $N_2/SF_6$  gas mixture) under the test conditions while  $CO_2/PFC$  gas mixture has the advantage over  $N_2/PFC$  gas mixture in terms of higher  $V_{PD}$ . The difference in  $V_B$  between  $N_2/PFC$  and  $CO_2/PFC$  gas mixtures may be attributed to the weaker electronegativity of  $N_2/PFC$  gas mixture which could reduce the shrinkage and heating of leader column and the activation of the streamer to leader transition [2] as well as the large electron scattering cross section of  $N_2$  which is more likely to retard electrons [1], resulting in increase of  $V_B$  even at higher gas pressures.

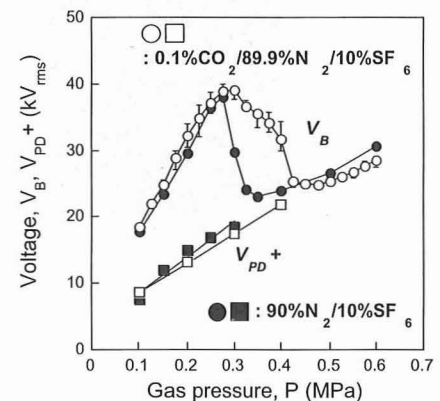
### 4.2 SYNERGY EFFECTS ON $V_{PD}$ AND $V_B$

In order to compare the synergy effects on  $V_{PD}$  and  $V_B$  between the  $N_2$  and  $CO_2$ -based gas mixtures including a PFC and  $SF_6$  gas in Figures 6 and 7, we introduce the index  $R_n$  (%) to quantify the degree of the synergy effect [7,8]. The index  $R_n$  is defined as equation (1).

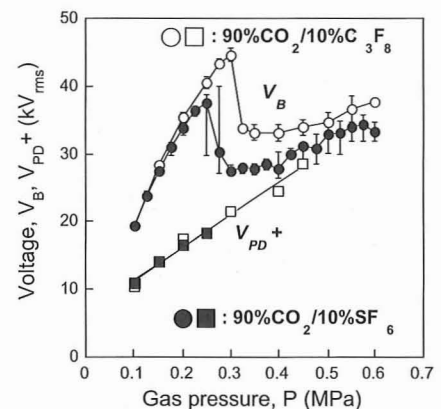
$$R_n = (V_S - V_r) / (V_1 - V_2) \times 100 \quad (1)$$



(a) Comparison between  $C_3F_8$  and  $SF_6$  gas in  $N_2$ -based gas mixture.



(b) Comparison between  $SF_6/CO_2$  and  $SF_6$  gas in  $N_2$ -based gas mixture.



(c) Comparison between  $C_3F_8$  and  $SF_6$  gas in  $CO_2$ -based gas mixture.

Figure 11. Difference in  $V_B$  vs  $P$  curves of  $N_2$  and  $CO_2$ -based gas mixtures with  $C_3F_8$  and  $SF_6$  gas.

where the subscript “*r*” of  $V_r$  is the mixture rate of PFC or SF<sub>6</sub> gas,  $V_1$  is measured  $V_{PD}$  of pure PFC or SF<sub>6</sub> gas ( $r = 100\%$ ) and  $V_2$  is also measured  $V_{PD}$  of the base gas of N<sub>2</sub> or CO<sub>2</sub> ( $r = 0$ ).  $V_r$  is  $V_{PD}$  at  $r\%$  when it is assumed that  $V_{PD}$  changes linearly with the mixture rate  $r$  between  $V_2$  and  $V_1$ , and  $V_S$  is measured  $V_{PD}$  at  $r\%$  ( $r$  is 10% in this study). When the synergy effect on  $V_B$  will be discussed, we can use the similar scheme as given in Figure 12 by changing the parameters with the corresponding  $V_{BS}$ .

Figure 13 indicates  $R_n$  of  $V_{PD+}$  at 0.2 MPa for N<sub>2</sub> and CO<sub>2</sub>-based gas mixtures including c-C<sub>4</sub>F<sub>8</sub>, C<sub>3</sub>F<sub>8</sub> and SF<sub>6</sub> gas.  $R_n$  for CF<sub>4</sub> gas mixtures is removed in the figure because  $V_S$  exceeded  $V_1$ ; i.e.  $V_{PD}$  of the CF<sub>4</sub> gas mixture did not obey Takuma’s equation [7,8]. Figure 13 indicates that  $R_n$  for CO<sub>2</sub>-based gas mixtures is larger than that for N<sub>2</sub>-based ones irrespective of the additive gas of PFC or SF<sub>6</sub> gas. This higher  $R_n$  of CO<sub>2</sub>/PFC gas mixtures than N<sub>2</sub>/PFC ones was also confirmed not only in other gas pressures at 0.15 and 0.25 MPa in our study, but also in other study on c-C<sub>4</sub>F<sub>8</sub> gas mixtures measured with the sphere to plane electrodes [7,8].  $R_n$  of  $V_{PD+}$  increases in order of gas mixture including c-C<sub>4</sub>F<sub>8</sub>, C<sub>3</sub>F<sub>8</sub> and SF<sub>6</sub> gas. It can be concluded from Figure 13 that the synergy effect on  $V_{PD+}$  for CO<sub>2</sub>-based gas mixtures is much larger than that for N<sub>2</sub>-based ones, and in terms of the additive gas, those for the PFC gas is smaller than that for SF<sub>6</sub> gas.

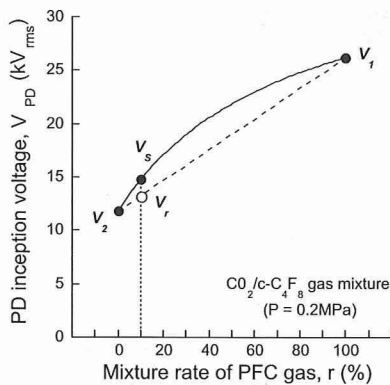


Figure 12. Parameters for index  $R_n$  of equation (1), explained using  $V_{PD}$  as an example. When  $R_n$  of  $V_B$  is estimated, these parameters are replaced with the corresponding  $V_B$ .

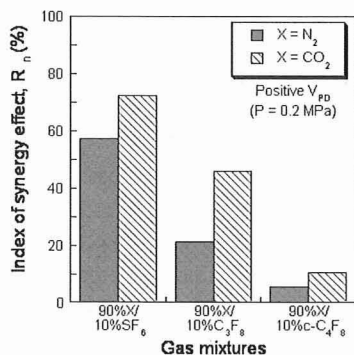


Figure 13.  $R_n$  of positive  $V_{PD}$  for different gas mixtures.

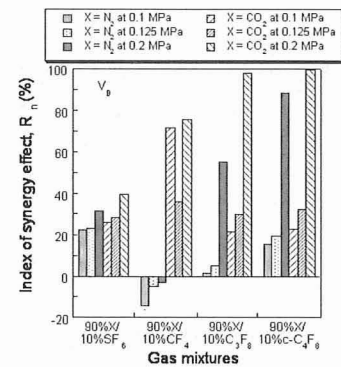


Figure 14.  $R_n$  of positive  $V_B$  for different gas mixtures.

Figure 14 shows  $R_n$  of  $V_B$  estimated at 0.1 and 0.125 MPa. These gas pressures were selected below  $P_m$  of unitary PFC gas to eliminate the corona stabilization effect as much as possible. It should be noted that only  $R_n$  for N<sub>2</sub>/CF<sub>4</sub> gas mixture shows negative value, which means the “negative” synergy effect. In Figure 14,  $R_n$  of  $V_B$  for CO<sub>2</sub>-based gas mixtures is larger than that for N<sub>2</sub>-based ones. This result is similar with that for  $V_{PD+}$  shown in Figure 13. Note that  $R_n$  of  $V_B$  at 0.2 MPa drastically rises to near 100% because  $V_B$  of the gas mixture becomes larger than that of the each unitary PFC gas. Consequently, the results in Figures 13 and 14 reveal that CO<sub>2</sub>-based gas mixtures have an advantage in terms of the synergy effect on both  $V_{PD+}$  and  $V_B$  as compared with N<sub>2</sub>-based ones.

### 5 CONCLUSION

Electrical insulation and discharge properties of N<sub>2</sub> and CO<sub>2</sub>-based gas mixtures including a PFC gas such as CF<sub>4</sub>, C<sub>3</sub>F<sub>8</sub> and c-C<sub>4</sub>F<sub>8</sub> gas were experimentally investigated under non-uniform field with ac high voltage application. As a result, it was found that gas pressure dependence of  $V_B$  for both N<sub>2</sub>/PFC and CO<sub>2</sub>/PFC gas mixtures showed the *N* shape characteristics but their  $V_B$  vs  $P$  properties were different.  $V_B$  vs  $P$  properties of CO<sub>2</sub>/PFC gas mixtures indicated the similarity of those of CO<sub>2</sub>/SF<sub>6</sub> gas mixtures.  $V_B$  properties of N<sub>2</sub>/PFC gas mixture were superior to those of CO<sub>2</sub>/PFC ones because of the higher  $V_B$  properties and the wider corona stabilization region even under gas pressures over  $P_m$ . On the other hand, in terms of  $V_{PD}$ , CO<sub>2</sub>/PFC gas mixtures had an advantage over N<sub>2</sub>/PFC ones due to higher  $V_{PD}$  that might contribute to the development of a new PFC gas insulated power apparatus with corona free design. The advantage of CO<sub>2</sub>/PFC gas mixtures was also found in the synergy effects on both  $V_{PD}$  and  $V_B$ , which were discussed by using the index  $R_n$  that quantifies the degree of the synergy effects. The synergy effect of CO<sub>2</sub>-based gas mixtures was larger than that of N<sub>2</sub>-based ones irrespective of the additive gas of the PFC (c-C<sub>4</sub>F<sub>8</sub> or C<sub>3</sub>F<sub>8</sub> gas) and SF<sub>6</sub> gas.

## ACKNOWLEDGMENT

The authors are grateful to Prof. M. Cho for his useful discussion on insulation properties of PFC gases. This study was supported in part by the Grant-in-Aid for Scientific Research from the Ministry of Education, Science, Sports and Culture, Japan and the Proposal - Based New Industry Creative Type Technology R&D Promotion Program from the New Energy and Industry Technology Development Organization (NEDO) of Japan.

## REFERENCES

- [1] L. G. Christophorou and R. J. van Brunst, "SF<sub>6</sub>/N<sub>2</sub> Mixtures Basic and HV insulation properties", IEEE Trans. Dielectr. Electr. Insul., Vol.2, pp.952-1003, 1995.
- [2] H. Okubo and N. Hayakawa, "Dielectric Characteristics and Electrical Insulation Design Techniques of Gases and Gas Mixtures as Alternatives to SF<sub>6</sub>", Gaseous Dielectrics X, pp.243-252, 2004.
- [3] T. Takuma, O. Yamamoto and S. Hamada, "Gases as Dielectric", Gaseous Dielectrics X, pp.195-204, 2004.
- [4] D. R. James, L. G. Christophorou, R. Y. Pai, M. O. Pace, R. A. Mathis, I. Sauers and C. C. Chan, "Dielectric strengths of new gases and gas mixtures", Gaseous Dielectrics I, pp.224-257, 1978.
- [5] J. C. Devins, "Replacement gases for SF<sub>6</sub>", IEEE Trans. Electr. Insul., Vol.15, pp.81-86, 1980.
- [6] S. Okabe, S. Yuasa and H. Suzuki, "Dielectric Properties of Gas Mixtures with Carbon Fluoride Gases and N<sub>2</sub>/CO<sub>2</sub>", Gaseous Dielectrics IX, pp.345-350, 2001.
- [7] O. Yamamoto, T. Takuma, S. Hamada and Y. Yamakawa, "Applying a Gas Mixture Containing c-C<sub>4</sub>F<sub>8</sub> as an Insulation Medium", IEEE Trans. Dielectr. Electr. Insul., Vol.8, pp.1075-1081, 2001.
- [8] O. Takenoshita, Y. Yamakawa, K. Obata, D. Akasaka, O. Yamamoto, S. Hamada and T. Takuma, "Dielectric strength of gas mixtures containing c-C<sub>4</sub>F<sub>8</sub>", J. Japan Research Group of Electrical Discharge, No.164, pp.109-112, 2000 (in Japanese).
- [9] S. Ohtsuka, M. Koumura, M. Cho, Y. Hashimoto, M. Nakamura and M. Hikita, "Insulation Properties of CO<sub>2</sub>/N<sub>2</sub> Gas Mixture with a Small Amount of SF<sub>6</sub>", Gaseous Dielectrics IX, pp.295-300, 2001.
- [10] N. Hayakawa, Y. Yoshitake, N. Koshino and H. Okubo, "Impulse Partial Discharge Propagation and Breakdown Characteristics in N<sub>2</sub>/SF<sub>6</sub> Gas Mixtures", Gaseous Dielectrics X, pp.87-92, 2004.



**Masayuki Hikita** (M'97-SM'98) was born in 1953. He received the B.S., M.S. and Dr. degrees in electrical engineering from Nagoya University of Japan, in 1977, 1979, and 1982, respectively. He was an Assistant Lecturer, a Lecturer, and an Associate Professor at Nagoya University in 1982, 1989, and 1992, respectively. Since 1996, he has been a Professor in the Department of Electrical Engineering, Kyushu Institute of Technology. He was a Visiting Scientist at the MIT High Voltage Laboratory in the USA, from August 1985 to July 1987. Dr. Hikita has recently been interested in research on the development of diagnostic techniques for electric power equipment. He is a member of the Japan Society of Applied Physics and the IEEJ.



**Shinya Ohtsuka** was born in Fukuoka on 16 January 1971. He received the B.Eng., M.Eng. and Dr. degrees in electrical and electronic engineering from Kyushu University, Japan, in 1993, 1995 and 1998, respectively. From 1996 to 1998, he was a research fellow of the Japan Society for the Promotion of Science. In 1999, he became an Assistant Professor in the Faculty of Engineering at Kyushu Institute of Technology, Japan. His research interests include the insulating properties of SF<sub>6</sub> gas, including diagnostic techniques to measure partial discharge in electrical power equipment and superconductors. Dr. Ohtsuka is a member of the Institute of Electrical Engineers of Japan (IEEJ), the Institute of Engineers on Electrical Discharges in Japan (IEEDJ) and Cryogenic Association of Japan.



**Shigemitsu Okabe** (M '98) was born on 18 September 1958. He received the B.Eng., M.Eng. and Dr. degrees in electrical engineering from the University of Tokyo in 1981, 1983 and 1986, respectively. He has been with the Tokyo Electric Power Company since 1986, and is presently group manager of the High Voltage & Insulation Group at the R & D center. He was a visiting scientist at Technical University of Munich in 1992. He has been involved in several research projects on transmission and distribution equipment. Dr. Okabe is a member of IEE of Japan.



**Shuhei Kaneko** was born on 11 February 1975. He received the B.S. and M.S. degrees from Keio University in 1998 and 2000, respectively. He joined the Tokyo Electric Power Company in 2000. Currently he is a researcher at the High Voltage & Insulation Group of the R&D Center and mainly engaged in research on GIS insulation. Mr. Kaneko is a member of IEE of Japan.